Measurement of the Reaction $\mu^-+C^{12}\rightarrow B^{12}+\nu^*$†

E. J. MAIER,‡ R. M. EDELSTEIN, AND R. T. SIEGEL§
Carnegie Institute of Technology, Pittsburgh, Pennsylvania
(Received 28 August 1963)

A measurement of the rates of negative muon absorption to particle-stable states of boron-12 has been performed with scintillation counters. In order to obtain the absorption rate to the ground state *alone*, a measurement was first performed of the absorption rate to all bound states of B^{12}. Separation of the contribution from absorption to B^{12} excited bound states was then effected by observation of coincidences between nuclear de-excitation gamma rays and the B^{12} ion recoiling after muon absorption. The measured rate for muon absorption to the ground state of B^{12} is (6750^{+300}_{-750}) sec^{-1}, in good agreement with prediction of the universal Fermi interaction.

I. INTRODUCTION

AMONG the three "classical" or strangeness-conserving weak interactions, negative muon absorption has been subject to the least quantitative experimental investigation. As a consequence, the coupling constants for muon absorption are at present known much less accurately than those in β decay and muon decay. The reasons for this comparative lack of information are not difficult to ascertain. Not only are muon sources weak, characteristically yielding stopping intensities of 5×10^2 to 5×10^4 per sec, but the absorption phenomenon for μ^- in mesic atoms of $A<12$ is rare, 10^{-1} to 10^{-3} compared to decay. For heavier nuclei, absorption does indeed compete with decay, and most experiments on μ^- capture have been performed on complex nuclei.[1] But attempts to obtain coupling constants by scanning the periodic table and applying closure results have encountered theoretical obstacles, not yet clearly overcome.[2] Experiments on absorption in liquid hydrogen[3] have not yet yielded results free of uncertainty in initial molecular state configurations. However, one expects that the most accurate coupling constants will proceed from measurements in light nuclei, particularly H, D, and He^3.

The experiment reported here is a measurement of the transition probability for the reaction

$$\mu^-+C^{12}\rightarrow B^{12}+\nu_\mu. \tag{1}$$

The rate for this process, involving a transition between an initial 0^+ nucleus and a final 1^+ nucleus, is determined by the *effective* coupling constants $\Gamma_A{}^\mu$, $G_A{}^\mu$, and $G_P{}^\mu$, where[1]

$$\begin{aligned}(\Gamma_A{}^\mu)^2&=(G_A{}^\mu)^2+\tfrac{1}{3}[(G_P)^2-2G_AG_P],\\ G_A{}^\mu&=g_A{}^\mu-(g_V{}^\mu+g_M{}^\mu)(\nu/2M),\\ G_P&=[g_P{}^\mu-g_A{}^\mu-g_V{}^\mu-g_M{}^\mu](\nu/2M).\end{aligned} \tag{2}$$

$g_A{}^\mu$, $g_P{}^\mu$, $g_M{}^\mu$, and $g_V{}^\mu$ represent the axial vector, pseudoscalar, weak magnetism, and vector coupling constants of muon absorption, respectively. Here ν is the neutrino momentum, and M the nucleon mass, so that $\nu/2M\approx0.05$.

We see that the effects on $\Gamma_A{}^\mu$ of the virtual pion terms represented by $g_P{}^\mu$ and $g_M{}^\mu$ are of the order of 30%, much larger than the corresponding effects in nuclear β decay. Accurate measurement of the rate of reaction (1) may thus serve to measure the virtual pion effects, if we assume $g_A{}^\mu$ to be already known from $\pi-e$ decay.[4] Unfortunately, the uncertainties in the nuclear matrix element which also enters into (1) makes it difficult to predict the rate more accurately than about 10%. This matter will be discussed in greater detail in Sec. IV.

The experimental determinations of the rate of reaction (1) have a long history, as muon physics goes. The first measurement, by Godfrey,[5] gave early evidence of the universal strength of weak interactions. Since then there have been five similar experiments,[6–10] which have

* Supported in part by the U. S. Atomic Energy Commission.
† Based on a thesis submitted by E. J. Maier in partial fulfillment of the requirements for the Ph.D. degree at Carnegie Institute of Technology.
‡ Present address: Goddard Space Flight Center, Greenbelt, Maryland.
§ Present address: The College of William and Mary, Williamsburg, Virginia.
[1] For recent reviews, see L. Wolfenstein, in *Proceedings of the 1960 Annual International Conference on High-Energy Physics at Rochester* (Interscience Publishers, Inc., New York, 1960), p. 529; and C. Rubbia, in *Proceedings of the Rutherford Jubilee International Conference*, edited by J. E. Birks (Heywood and Company Ltd., Manchester, 1962), p. 707. The most comprehensive paper on muon capture is H. Primakoff, Rev. Mod. Phys. **31**, 802 (1959). Virtual pion effects are discussed by M. Goldberger and S. Treiman, Phys. Rev. **111**, 355 (1958); and L. Wolfenstein, Nuovo Cimento **8**, 882 (1958).
[2] R. Klein and L. Wolfenstein, Phys. Rev. Letters **9**, 408 (1962); J. R. Luyten, H. P. C. Rood, and H. A. Tolhoek, Nucl. Phys. **41**, 236 (1963).
[3] R. Hildebrand, Phys. Rev. Letters **8**, 34 (1962); E. Bleser, L. Lederman, J. Rosen, J. Rothberg, and E. Zavattini, Phys. Rev. Letters **8**, 288 (1962); E. Bertolini, A. Citron, G. Gialanella, S. Focardi, A. Mukhin, C. Rubbia, and S. Saporetti, *Proceedings of the 1962 Annual International Conference on High-Energy Physics at CERN*, edited by J. Prentki (CERN, Geneva, 1962).
[4] A. Strelzoff, L. Pondrom, R. Garland, and E. Dicapua, Bull. Am. Phys. Soc. **8**, 481 (1963); H. L. Anderson, T. Fujii, R. H. Miller, and L. Tau, Phys. Rev. **119**, 2050 (1960).
[5] T. N. K. Godfrey, thesis, Princeton University, 1954 (unpublished).
[6] J. O. Burgman, J. Fischer, B. Leontic, A. Lundby, R. Meuhler, J. P. Stroot, and J. D. Teja, Phys. Rev. Letters **1**, 469 (1958); J. D. Teja, Arch. Sci. (Geneva) **12**, 131 (1959).
[7] B. L. Bloch, thesis, Carnegie Institute of Technology, Report NYO-9280, 1960 (unpublished).
[8] H. V. Argo, F. B. Harrison, H. W. Kruse, and A. J. McGuire, Phys. Rev. **114**, 626 (1959).
[9] J. G. Fetkovich, T. H. Fields, and R. L. McIlwain, Phys. Rev. **118**, 319 (1960).
[10] G. T. Reynolds, D. B. Scarl, R. A. Swanson, J. R. Waters, and R. A. Zdanis, Phys. Rev. **129**, 1790 (1963).

varied in their results far beyond the quoted errors. The Los Alamos group[8] used cosmic-ray muons, while the others have used cyclotron produced particles. It was our purpose to improve upon an earlier experiment performed at this laboratory[7] in order to resolve the discrepancies among reported results.[11]

It is interesting that only reaction (1) has been studied experimentally among all possible pure Gamow-Teller muon-capture reactions to a final nucleus ground state. The reasons for this are both theoretical and experimental. On the theoretical side, other reactions to a ground state such as $\mu^-+Li^6 \rightarrow He^6+\nu$ have been found to have rates which depend very sensitively on nuclear properties,[12] so that this measurement would yield more information about nuclear physics than about muon physics.

From the experimental point of view, B^{12} is almost uniquely suited for detection by means of the energetic (13.5-MeV end point) beta rays emitted in the radioactive decay back to C^{12}. The short mean-life (29.3 msec) for this decay is an order of magnitude smaller than that of any other muon-absorption end product. This minimizes the time during which a search is made for delayed activities, and thus minimizes random background. It is this fact which has made the reaction (1) readily accessible to detection via the delayed activity. Reactions with lighter nuclei are detectable by direct observation of the recoil nucleus, as is the case in hydrogen and helium-3 (see Sec. III in this connection).

There is an experimental difficulty with regard to reaction (1), which is associated with the existence of bound excited states of B^{12}. Muon absorption directly to these excited states will produce B^{12} in its ground state following electromagnetic de-excitation, and B^{12} nuclei formed in this way will form a contribution to the delayed activity measured. That is,

$$\begin{aligned} \mu^-+C^{12} &\rightarrow B^{12*}+\nu \\ &\quad\big\lfloor\rightarrow B^{12}+\gamma. \end{aligned} \tag{1a}$$

Analysis indicates[5] that 10–20% of all absorptions should proceed via the excited states, but the computations are approximate. The Los Alamos group found that about 10% of their B^{12} events were associated with prompt signals, apparently from the γ rays of reaction (1a). It has therefore become customary to make a 10% correction for the excited states after measuring the total B^{12} activity produced by muons in carbon. As a second part of the present experiment, we undertook to detect the reaction (1a), and report the results in Sec. III.

In Sec. II we describe in detail the detection of all B^{12} nuclei formed by μ^- in carbon, i.e., the sum of reaction rates for (1) and (1a). In Sec. III the experiment to measure excited state contributions is described, and in Sec. IV the results are discussed.

II. ABSORPTION TO ALL BOUND STATES

A. Beam and Counter Geometry

We define $\lambda_B{}^{\text{total}}$, the absorption rate to *all* bound states of B^{12} via reactions (1) and (1a). The measurement of $\lambda_B{}^{\text{total}}$ is performed by determining the number N_B of B^{12} nuclei associated with the decay of a known number of N_μ of muons in a plastic (CH) scintillant. (More than 99% of stopped muons form carbon mesic atoms.) The rate $\lambda_B{}^{\text{total}}$ is given by $\lambda_B{}^{\text{total}}=\lambda_{\text{decay}}\times N_B/N_\mu$, where λ_{decay} is the decay rate of a muon in the 1S orbit of the carbon mesonic atom. λ_{decay} differs by less than $\frac{1}{4}$% from the free muon decay rate,[13] so that $\lambda_{\text{decay}}=1/2.20\times10^6$ sec^{-1}.[14]

The muon beam was the 48-MeV "pure" muon beam of the Carnegie cyclotron. It was produced by the decay in flight of 115-MeV pions emerging from the shielding wall, the muons being emitted at 180° to the pion direction in the c.m. system. In this "backward" beam, the muons are thus polarized oppositely to those in the usual "forward" muon beams. This was confirmed by

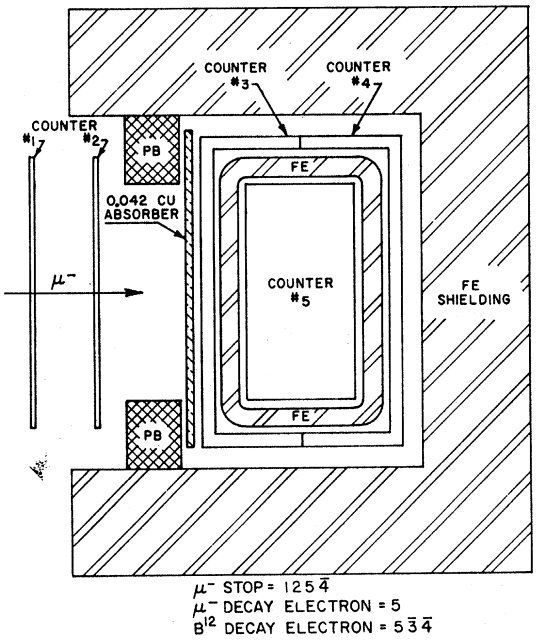

FIG. 1. Experimental geometry for measurement of muon absorption to all B^{12} bound states—horizontal section.

[11] The results of the total B^{12} production part of the present experiment (cf. Sec. II) were given in E. J. Maier, B. L. Bloch, R. M. Edelstein, and R. T. Siegel, Phys. Rev. Letters **6**, 417 (1961); cf., E. J. Maier, thesis, Carnegie Institute of Technology Report NYO-9287, 1962 (unpublished).

[12] H. Überall, Carnegie Institute of Technology Report NYO-2236, 1959 (unpublished).

[13] H. Überall, Phys. Rev. **119**, 365 (1960); D. Yovanovitch, *ibid.* **117**, 1580 (1960).

[14] R. A. Lundy, Phys. Rev. **125**, 1686 (1962); M. Eckhause, Carnegie Institute of Technology Report NYO-9268, February 1962 (unpublished); see also F. J. M. Farley, *Proceedings of the 1962 Annual International Conference on High-Energy Physics at CERN*, edited by J. Prentki (CERN, Geneva, 1962), p. 415.

decay asymmetry measurement. Studies with a star counter established the pion contamination of the pure negative muon beam as $\frac{1}{3}\%$.[15]

Figure 1 shows the counter geometry. All counters were of Pilot B scintillating plastic. The muons passed into the apparatus through a 4-in. square hole in a 4-ft-thick steel and lead blockhouse wall, and were brought to rest in counter No. 5 by the copper and iron absorber. In order to stop the beam in the center of No. 5, the 0.375-in.-thick iron box was removed, a range curve taken with copper absorber, and the iron box then put in place with a reduced amount of copper.

The aperture in the lead window following counter No. 2 was varied from 4-in.×4-in. to a 3-in.-diam circle or a 2-in.-diam. circle at different stages of the experiment. This variation in beam area made possible a check of the corrections applied to the observed B^{12} rate, as will be discussed below.

The 0.375-in. Fe shield box prevented B^{12} decay electrons emitted from counter No. 5 from activating the anticoincidence counters No. 3 and No. 4, and vice versa. Calculation indicates that fewer than 0.3% of all such electrons traversed this box via an $e-\gamma-e$ bremsstrahlung reconversion mechanism.

Counter Nos. 1 and 2 were 5 in.×$5\frac{1}{4}$ in.×1/16 in., and were viewed by 6810A photomultipliers, as were No. 3 and No. 4. The latter two counters were constructed of $\frac{1}{4}$-in. plastic sheet and were shaped to surround counter No. 5 as completely as possible. Figure 1 is a horizontal section through the apparatus, and above this array counter Nos. 3 and 4 were closed to form an anticoincidence roof to protect against cosmic rays. Thus, the combination $5\,\bar{3}\bar{4}$ showed a (cyclotron off) rate of ~2/min, more than an order of magnitude reduction below the rate in No. 5 alone. The counter Nos. 3 and 4 were optically independent, so that No. 4 could also be used in the beam monitoring telescope $12\bar{5}\bar{4}$.

The counter No. 5 was 4-in.×4-in.×2-in. thick, and was viewed through a $1\frac{1}{4}$-in.×2-in.×4-in. Vycor (SiO_2) light pipe by two 6292 photomultipliers. Extensive tests were made with collimated x-ray sources to insure optimal resolution, and uniformity of pulse height to within 10% over the entire volume of this counter. The Vycor light pipe was necessary to achieve this end. Tests with reduced beam area confirmed that muon-decay electrons from the oxygen in the Vycor produced no contamination in the geometry used.

Two signals were taken from counter No. 5. First, the anodes of the two P.M. tubes were joined and loaded with 100 Ω to obtain a fast output pulse. The last dynodes were also joined, loaded with a high (250 kΩ) resistor, and fed to a cathode follower. This slow output was used in establishing pulse-height discrimination.

[15] F. Ajzenberg-Selove and T. Lauritsen, Nucl. Phys. **11**, 1 (1959).

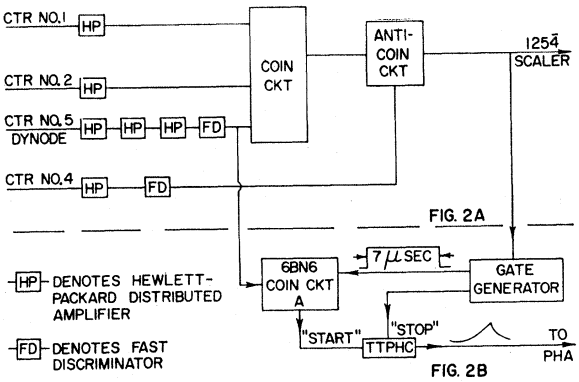

FIG. 2. Electronics block diagram for measurement to all B^{12} bound states. Figure 2A is the Monitor circuit. Figure 2B is the muon-decay time analyzer.

B. Electronics

The detection circuitry consisted of three sections: the beam monitoring circuit, the muon-decay time analyzer, and the B^{12} decay time analyzer. Block diagrams are shown in Figs. 2 and 3. The monitor coincidence circuit (Fig. 2A) was of Garwin type and was operated with a resolving time of 15 nsec, the discriminator threshold on No. 5 being set at less than 0.5 MeV.

The muon-decay electron time distribution was measured relative to the stopping signal $12\bar{3}\bar{4}$ by means of a commercial (Eldorado) time-to-pulse height converter (TTPHC). The TTPHC was started by a delayed event in counter No. 5, and stopped by a pulse derived from the trailing edge of the 7-μsec gate (see Fig. 2B), thus producing a rising exponential time spectrum to be stored in the PHA.

For the B^{12} decay part of the experiment, the cyclotron operation was altered from its usual rate of 205 FM pulses per sec. This was done in order to allow the B^{12} rate to (a) build up during a period comparable to its mean life, and (b) decay during a period greater than three mean lives during which the cyclotron was off, so that background was minimized. The cyclotron tim-

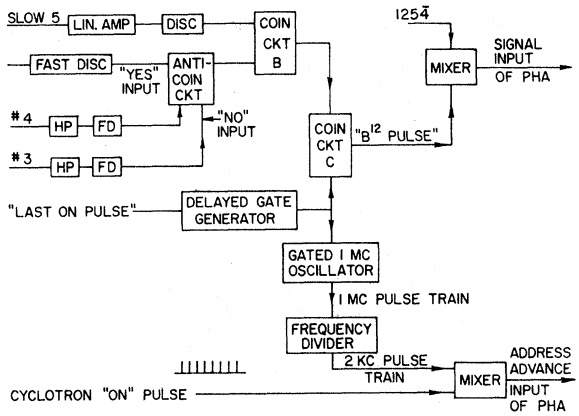

FIG. 3. Block diagram of B^{12} decay time analyzer.

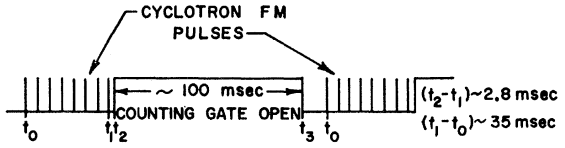

FIG. 4. Timing sequence of cylotron pulses for measurement to all B^{12} bound states.

ing sequence is shown below in Fig. 4. In this sequence, the muons produced B^{12} during each of the eight beam bursts, which were not necessarily of equal intensity. This inequality required monitoring of the number of stopping signals $123\bar{4}$ in each of the eight beam bursts, thus permitting calculation of an effective source strength at time t_2, the beginning of the B^{12} detection interval.

Time analysis of the B^{12} pulses and scaling of the stop pulses $125\bar{4}$ in each FM pulse were accomplished by modifying the RCL-256 channel analyzer used previously for the muon-decay measurement. The memory control circuit was changed so that the memory address could be incremented by external command, and could also be reset to address 1 by external command. Then the instrument became a time analyzer in that it added to the number in channel "n" the number of pulses arriving at its input while it was at address n. Figure 3 shows the circuitry which advanced the memory address to perform the dual functions required. From t_0 to t_1 the memory address was advanced from channels 2 through 9, remaining at each address 5 msec during which one acceleration cycle was completed in the cyclotron. Addresses 2 through 9 registered the number of stopping particles occurring during FM pulses 1 through 8, respectively. The analyzer remained at address 9 until time t_2. At time t_2 the same gate used for the B^{12} time condition turned on a 1-Mc oscillator which produced via a sequence of frequency dividers a 100 msec long train of pulses spaced accurately at $\frac{1}{2}$ msec intervals. These advanced the memory through address 10 to 210 during time interval t_2 to t_3, remaining at each address $(\frac{1}{2}-\gamma)$ msec, where γ is the deadtime required for the advance operation. At time t_3 a pulse derived from the trailing edge of the 100-msec B^{12} coincidence gate reset the memory address to 1, where it remained until the start of the next complete cycle. Thus, each of channels 10 through 210 counted the number of B^{12} decays occurring during a $\frac{1}{2}$-msec-wide interval at a fixed time relative to the time of the last of the 8 cyclotron FM pulses. The contents of the analyzer memory were printed out after counting intervals of the order of an hour.

TABLE I. Conditions under which B^{12} data were recorded during measurement of absorption to all bound states.

Condition	Disc. cutoff (MeV)	Collimator size (in.)	Beam area (in.²)	Beam intensity
1	2.3	2	3	Maximum
2	1.5	2	3	Maximum
3	2.3	3	7	Maximum
4	1.5	3	7	Maximum
5	1.5	4	16	Maximum
6	2.3	4	16	Maximum
7	2.3	4	16	$\frac{1}{2}$
8	2.3	4	16	$\frac{1}{4}$
9	2.3	4	16	[a]
10	1.5	4	16	[a]

[a] Maximum; deflecting magnet off: $\frac{3}{4}$-in. Pb absorber on beam line to absorb charged particles.

C. Analysis of B^{12} Decay Data

The delayed activities produced in counter No. 5 were studied under the ten different conditions listed in Table I. The B^{12} data consisted of the first eight groups of data, the last two conditions giving background only. For each of the first eight groups a least-squares analysis was made of the time spectra which appeared in the PHA channels 10–210. The best fit of each group to the theoretical curve $xe^{-n\lambda}+y$ was obtained, where n is the channel number and $\lambda=1/29.3$ msec^{-1} is the currently accepted decay rate of B^{12}.[15] A sample of such data with the fitted curve is shown in Fig. 5, where the points each contain the data from 10 channels.

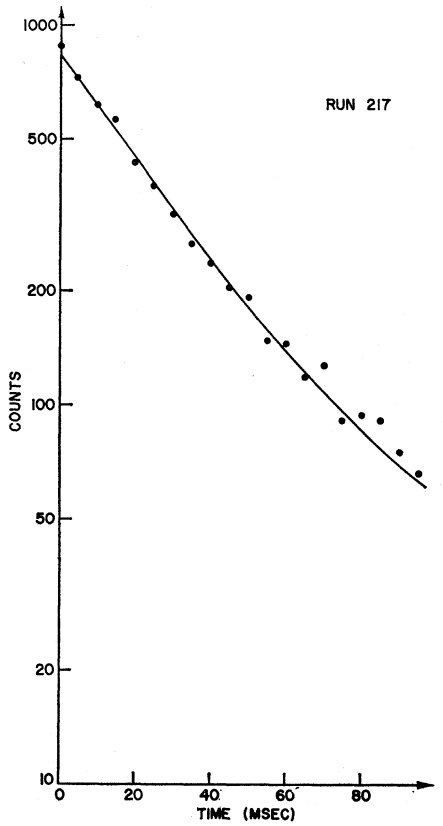

FIG. 5. Sample of B^{12} decay data (Run No. 217). Solid dots are experimental points. Curve is result of least-squares fit, which yielded for this run $C=761.4\exp(-t/29.3)+30.6$.

Analyses were performed for each group of data using the counts obtained in intervals t to t_3, where t was varied from (t_2+0.5 msec) to (t_2+40.5 msec) in steps of 5 msec. This changed the included time from a maximum of 100 msec to a minimum of 60 msec. The amplitude x of the exponential starting at t was then corrected upward to give an amplitude at time (t_2+0.5 msec). These values could then be compared to detect any short-lived activity which might be present at early times. A sample of the results of this procedure is shown in Fig. 6, and indicates that such short-lived activity was indeed present. The "correct" amplitude for the B^{12} activity in each of the eight data groups was chosen as that amplitude computed with t equal to 5 msec plus the time at which the amplitude versus t curve was judged to have reached its asymptotic value.

There are several reasons to attribute this apparent time dependence of the amplitude ("amplitude effect")

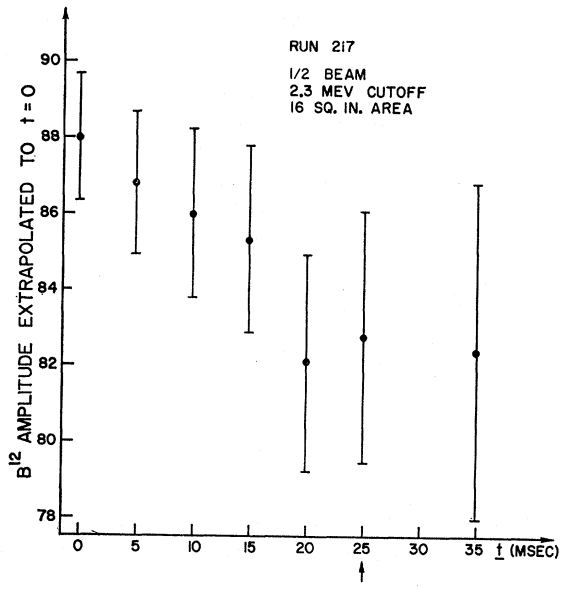

FIG. 6. Sample of "amplitude effect" in B^{12} (see text).

to a short-lived component, rather than to a systematic error which might effect all the data in some unknown fashion. First, a 5 msec component was clearly observed in preliminary cyclotron runs using only a single FM burst before each B^{12} counting interval. Such effects have also been observed at other laboratories.[6] Second, reducing the beam area made our "amplitude effect" worse, so that the apparent amplitude change persisted as long as 40 msec in the case of the smallest (2-in.-diam) beam used. This clearly indicates an effect associated with the general cyclotron level, and not with the incident muon beam. Third, the amplitude effect was discovered by noting that when all B^{12} time data were used in the least-squares analysis, the background amplitude y consistently appeared to be less than the cosmic-ray and radioactive background (~2/min) in counter No. 5, measured before and during each cyclotron run. This anomaly disappeared when the asymptotic amplitude was obtained as described above, and we found that the machine-off background then came into excellent agreement with the measured y.

TABLE II. Results (f) of fitting B^{12} decay data obtained under the first eight conditions of Table I.

Condition	$f \times 10^2$	$\Delta f/f$[a] (%)
1	0.8376	6.04
2	0.8703	6.44
3	1.0076	2.10
4	1.0269	2.26
5	1.0138	2.16
6	1.0275	1.97
7	1.006	3.96
8	0.9686	2.77

[a] Errors are from statistics of B^{12} amplitude only.

It is worth noting that a lifetime search of the data did *not* serve to detect the short-lived component. For this lifetime study all eight data groups were combined in order to obtain reasonable statistics. The result was that the mean life increased from 28.8±0.6 msec to 30.25±1.6 msec as the first 10 msec or first 30 msec were excluded from the fitting program. Either value is in good agreement with the 29.3 msec accepted,[15] so that it was not possible to detect a short-lived component by this method. In addition, the observed values of χ^2 were all such as to be acceptable, giving no clear indication of a short-lived component. Finally, the insensitivity of the computed amplitude x to the assumed lifetime was so slight as to make errors in assumed B^{12} lifetime or time scale of small importance. In fact, a study of a typical data group (3-in. collimator, 2.3 MeV=E_{min}) showed that a 10% change in assumed B^{12} lifetime produced a 1.3% change in amplitude x.

We thus obtained for each group of data the best value for x, the number of B^{12} decays per $\frac{1}{2}$-msec interval beginning at (t_2+0.5 sec). From this we found by straightforward procedure f, the probability per unit monitor ($12\bar{3}4$) for production of a single B^{12} nucleus by particles stopping at (t_2+0.5 sec).

Table II lists the values of f for the first eight conditions in Table I. The errors listed are those from the statistics of the fitted amplitudes only.

Corrections were straightforward to calculate for the portion of the B^{12} β spectrum which escaped counter No. 5 without being detected. The observed insensitivity of the final B^{12} production rates to the magnitude of these corrections, which ranged from 1.02 to 1.15, indicated that they were accurately obtained by calculation.

Data taken in the 9th and 10th conditions listed in Table I permitted evaluation of the B^{12} production from fast neutrons via $C^{12}(n,p)B^{12}$. The upper limits for these two conditions for neutron-produced B^{12}, with E_{min}=1.5 MeV and E_{min}=2.3 MeV, were (0.6±1.0)% and (1.2±0.8)% with respect to B^{12} produced by muons,

It was difficult to ascertain whether the second value was the result of a short-lived activity or not, and in any event this source of background is negligible.

D. Analysis of Muon-Decay Data

The muon-decay curves were obtained from the TTPHC and a least-squares analysis performed. The assumed form of the data was again $(x=e^{-\lambda t}+y)$, where x is the best fit of μ-decay events corresponding to the first channel considered in a particular group of data. The various effects on this form produced by background rates and the nature of the TTPHC measurement[15] were negligible ($<1\%$) here. In analogy with the B^{12} decay measurement, we define g as the number of muons per unit monitor ($125\bar{4}$) which emit decay electrons.

A total of seven muon-decay runs of data was obtained with the three different collimator sizes. These runs were analyzed separately, and after observing their interval consistency, those within each collimator size group were combined to give three different values for g. The data were checked for contamination by eliminating early time channels in the manner described for the B^{12} time data, but no amplitude effect was observed here. The values obtained for g are listed in Table III.

The errors listed are statistical only. In addition,there are errors assigned to the parameters used to calculate the values of g, as listed in Table IV. Compounding these, we find a net systematic error in g of 2.12%.

As in the case of the B^{12} data, a lifetime search of the muon time data was performed. If the data from the first 0.36 μsec following the stopping event were excluded, the mean life obtained for muons in carbon was (2.01 ± 0.04) μsec. Excluding the first 1.07 μsec yielded a value (2.09 ± 0.06) μsec. Either result agrees well with the accepted value of (2.043 ± 0.003) sec.[16]

E. Result

Using the values for f and g in Tables II and III, we evaluate the ratio f/g under each of the eight experimental conditions. These values are shown in Fig. 7, and all are observed to be in good agreement with each other. Each value has an error which was compounded from (a) statistical errors; (b) estimates of systematic errors in the B^{12} evaluation, which averaged $\sim4\%$, with the largest (3%) contribution from the surface escape correction; and (c) the systematic error in muon rate evaluation, about 2.1%.

The final value of the ratio $B=f/g$ was obtained by mixing the eight independent measurements with their statistical and spectrum escape errors only, then compounding in the final result the systematic errors which applied to all measurements. We obtain $B=(1.55\pm0.06)\times10^{-2}$.

[16] R. A. Reiter, U. S. Atomic Energy Commission Report NYO-9279, 1960 (unpublished).

TABLE III. Results of fitting muon-decay data for the three categories of muon-decay data. Errors indicated are statistical only.

Run	g	g-weighted mean
3-in. collimator:		
235	0.6714	
236	0.6882	0.6746 ± 0.0060
237	0.6704	(0.89%)
128	0.6626	
4-in. collimator:		
126	0.6163	0.6226 ± 0.0081
127	0.6288	(1.30%)
2-in. collimator:		
129	0.5991	0.5991 ± 0.0090 (1.66%)

The error evaluated from the variance of the eight measurements is 0.028×10^{-2}, indicating a conservative assignment of error in the value above.

III. ABSORPTION TO EXCITED STATES OF B^{12}

A portion of the B^{12} formed by muon absorption in carbon is formed in excited bound states, via reaction (1a). Four such bound states are known (see Fig. 8), and γ rays have been observed from the 0.95- and 1.67-MeV states. The γ rays are emitted promptly upon the muon absorption, and thus should exhibit a time spectrum relative to the stopping muon with 2.04-μsec mean life.

There is another source of γ rays with such a time distribution, namely,

$$\begin{aligned}\mu^-+C^{12}&\rightarrow B^{12*}+\nu\\ &\quad\downarrow\\ &\rightarrow B^{11*}+n\\ &\quad\downarrow\\ &\rightarrow B^{11}+\gamma.\end{aligned}\tag{5}$$

This process of muon absorption to unbound B^{12} states is about two orders of magnitude more intense than reaction (1a).

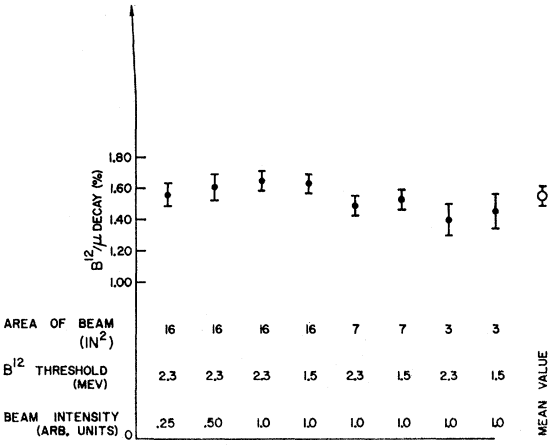

FIG. 7. Results for production of B^{12} in all bound states, measured under eight different experimental conditions.

The detection of process (1a) was accomplished by observing *each one* of the following sequence of events.

Event	Energy spectrum	Time spectrum relative to preceding event
$(e1) \equiv 1254$	>0.3 MeV in No. 5	Fast (10^{-8} sec) coinc.
$(e2) \equiv \mu^- + C^{12} \rightarrow C^{12*} + \gamma$	B^{12*} recoil energy = 375 keV	$\tau = 2.04$ μsec.
$(e3) \equiv B^{12*} \rightarrow B^{12} + \gamma$	γ-ray energy = 0.95, 1.67, 2.62, or 2.72 MeV	Fast (2×10^{-8} sec coinc).
$(e4) \equiv B_{gnd}^{12} \rightarrow C^{12} + e^- + \nu$	B^{12} β spectrum	$\tau = 29.3$ msec.

The detection of the stopping event ($e1$) was made with the same apparatus as in experiment I. Detection of event ($e2$) made the experiment feasible, and was accomplished by making use of a liquid scintillant in counter No. 5, and detecting the recoil B^{12} ion from the absorption event (cf., IIIB). Event ($e3$) occurred in rapid succession after event ($e2$) and the γ ray emitted was observed in a 6-in.-diam.$\times$3-in.-thick NaI(Tl) crystal. A fast coincidence (20 nsec) between events ($e2$) and ($e3$) suppressed all backgrounds except that from reaction (5). Finally, the requirement of a delayed B^{12} β ray helped to suppress reaction (5). If the various

TABLE IV. Errors involved in evaluation of muon-decay data.

Parameter	Error
Zero-time determination	0.7%
Scale factor (A)	2.0%
Other corrections	0.2%

energies were as predicted, if the time spectrum of ($e2-e3$) coincidences would be that of muon disappearance in carbon, and if a subsequent β decay was observed, we could be reasonably sure that an event from reaction (1a) was being detected.

A. Beam and Counter Geometry

The beam was identical to that used in experiment I, except that it was "stretched" by means of a rotating target inside the cyclotron. This improved the duty factor by a factor of 10, producing FM bursts about one msec in length rather than the 100 μsec bursts obtained previously.

Figure 9 shows a vertical section through the counter arrangement, which was similar to that used in experiment I, with two differences. First, the shield counter Nos. 3 and 4 assembly was mounted horizontally to allow detection of γ rays emerging downwards, the iron shield having been provided with an opening at the bottom. Second, a 6-in.-diam$\times$3-in.-thick NaI(Tl) crystal was mounted beneath the counter No. 5, to detect the deexcitation γ rays. This counter No. 6 was a Harshaw assembly viewed by three 6363 phototubes,

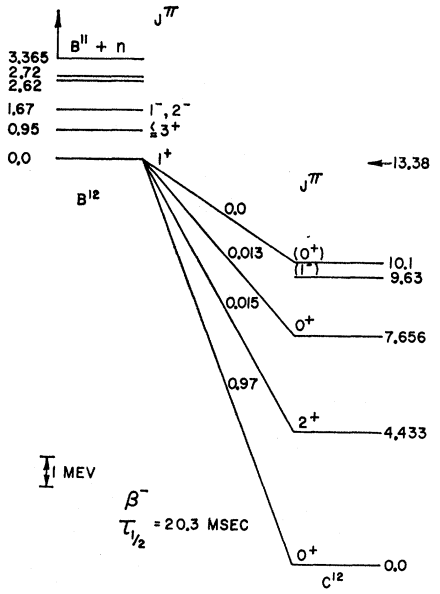

FIG. 8. B^{12} excited states and decay scheme. (From Ref. 15.)

and showed a 9% resolution (FWHM) with Cs^{137} γ rays. The crystal face was one inch below the counter No. 5.

Counter No. 7 was an anticoincidence guard for the NaI(Tl) crystal. It was a right cylinder 20 in. in diameter and 24 in. high, with an 8-in.-diam well 12 in. deep to contain counter No. 6. This large plastic scintillant was viewed by nine 6364 phototubes distributed on its top and bottom surfaces. It served to suppress Compton events in No. 6, background in No. 6 from high-energy (>2.7 MeV) γ rays, and also charged particle background.

The entire apparatus was shielded by an 18-in. paraffin layer, supplemented by a 1-in. layer of boric acid in an attempt to reduce neutron capture γ rays. The usual steel and concrete blockhouse was also present.

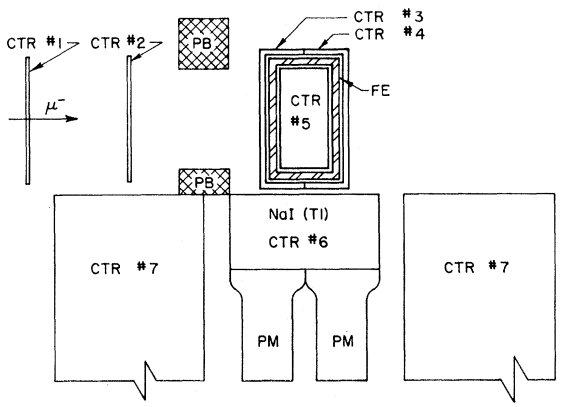

FIG. 9. Experimental geometry for measurement of muon absorption in carbon to form *excited* states of B^{12}.

B. Detection of B^{12*} Recoil and De-Excitation γ Rays

The energy of the recoil in reaction (1a) is about 375 keV, virtually the same as that of the ground state B^{12} nucleus recoiling from reaction (1). Its detection in an organic (CH) scintillator was made difficult by two factors. First, the intense specific ionization of such an ion saturates the luminescent centers along the path, and greatly reduces the scintillation light output compared to that of an electron of the same energy. Second, the large light pulse from the stopping muon must have disappeared before the absorption event occurs, and the electronic system must also have recovered.

The task of estimating the scintillation pulse height produced by the recoil ion was complicated by a lack of experimental information on the behavior of such ions. By using the data of Wright[17] and Zimmerman[18] and the stopping-power data of Powers and Whaling,[19] we concluded that the B^{12} ion should yield a scintillation pulse equivalent to that of a 5–7-keV electron. The most optimistic assumptions indicate that 15 keV might be obtained. Thus, the recoil detection system must be capable of seeing a 5-keV electron one microsecond after a stopping muon leaves 20 MeV in the target counter. Since Harrison[20] measured a slow component amplitude in the microsecond region equal to several percent of the total light emission for plastic scintillants, but observed $<0.1\%$ of such component for liquids, we chose a toluene based liquid scintillant for the counter No. 5 during experiment II. The liquid was contained in a stainless steel 4-in.×4-in.×2-in. cell, and viewed by two photomultipliers. The acceleration voltages were adjusted on the last few dynodes so that the saturated anode output corresponded to a 300-keV energy loss; but the tube operation was linear in the region below 50 keV in which the recoil ion peak was expected to occur.

The recoil detection counter No. 5 was placed in fast coincidence with the NaI(Tl) counter No. 6. (The circuitry is described in greater detail in the next section.) Tests were then made with the aid of radioactive test sources to ascertain the performance of this part of the counting system. Three sources were used to simulate the recoil $-\gamma$ phenomenon which was to be studied. Their characteristics are summarized in Table V.

Calibrated (10% accuracy) sources were obtained in the form of water solutions and also in the form of organic liquids containing soluble salts of the active isotopes. The water solutions were placed in the volume of counter No. 5 normally occupied by liquid scintillant, in order to measure the product of solid angle and photopeak efficiency of counter No. 6 for the nuclear γ rays listed in Table V. The values obtained for Zn^{65} and Y^{88} γ rays are shown in Fig. 10. The smooth curve is the result of a theoretical calculation of the efficiency of counter No. 6, averaged over the geometry of the source in No. 5, and corrected by a factor of 0.5 to account for absorption in the counter No. 5 and intervening layers of material between Nos. 5 and 6. This absorption factor is difficult to estimate. However, the *relative* efficiencies for No. 6 which were measured experimentally are in agreement with the shape of the theoretical curve, which was then used to obtain the efficiencies at the energies of 0.95, 1.67, and 2.7 MeV for the B^{12*} γ rays.

The organic source solutions of Zn^{65} and Y^{88} were dissolved in the scintillant of counter No. 5 for the final tests of the system. The pulse-height spectra in No. 5 obtained for the 8- and 16-keV x rays are shown in Fig. 11, curves A and B. Curves C and D are the Poisson distributions which best fit these measured curves and curve E is the expected spectrum for 5-keV recoil energy. Including the result of a coincidence circuit efficiency measurement with a recoil-γ resolving time of 25 nsec,

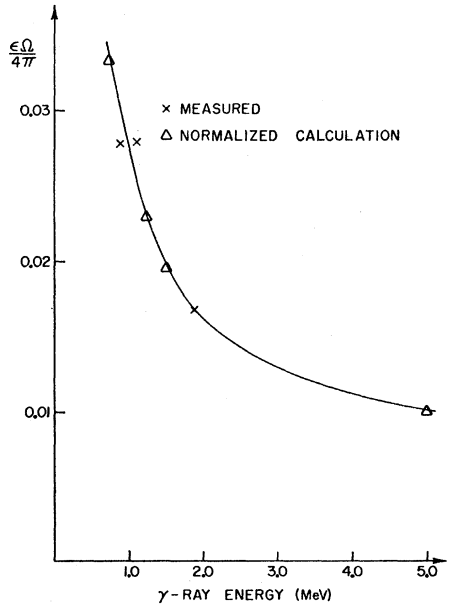

FIG. 10. Experimental and calculated (normalized) values for the product of photopeak efficiency and solid angle for a 6-in.×3-in. NaI(Te) counter viewing a 4-in.×4-in.×2-in. distributed source in the geometry of Fig. 9.

TABLE V. Properties of radioactive sources used in calibration of apparatus for excited B^{12} state measurement.

Parent	Nuclear γ-ray energy	K x-ray energy
Zn^{65}	1.11 MeV	8
Y^{88}	0.91	15
	1.84	
Ce^{139}	0.166	32

[17] G. T. Wright, Phys. Rev. **91**, 1282 (1953).
[18] E. J. Zimmerman, Phys. Rev. **99**, 1199 (1955).
[19] R. D. Powers and W. Whaling, Bull. Am. Phys. Soc. **6**, 519 (1961).
[20] F. B. Harrison, Nucleonics **12**, No. 3, 24 (1952).

we obtain a recoil detection efficiency of (0.75 ± 0.25) for any recoil energy equivalent between 5 and 50 keV.

C. Electronics

The monitor telescope was basically the same as in experiment I. Figure 12 is a block diagram of this portion of the electronics, which generated a signal for each particle stopped in counter No. 5 or the iron shield downstream from it. Those stopping events which occurred within the stretched portion of the beam were selected by a 1.5-msec-wide gate (coincidence circuit D), and designated as "stretched muons." Each stretched muon generated a delayed gate, the "muon gate," which defined the time limits for acceptance of a recoil coincidence. The trailing edge of the muon gate was used to generate the "TIM stop" signal, serving to close the time interval meter gate if a recoil-γ coincidence had opened it.

The recoil-γ detection circuitry is shown in Fig. 13. A fast gamma-ray pulse was obtained by zero-crossing technique, and placed in coincidence with counter No. 5 anode output. This fast coincidence opened a linear gate which allowed the linear pulse from No. 5 to pass into a fast single-channel analyzer which was constructed of two 10 Mc/sec discriminators. Pulses in No. 5 between 2.6 and 40 keV were accepted by this system, and placed in anticoincidence with the output from counter Nos. 3, 4, and 7, which suppressed background of charged particles and some neutrals.

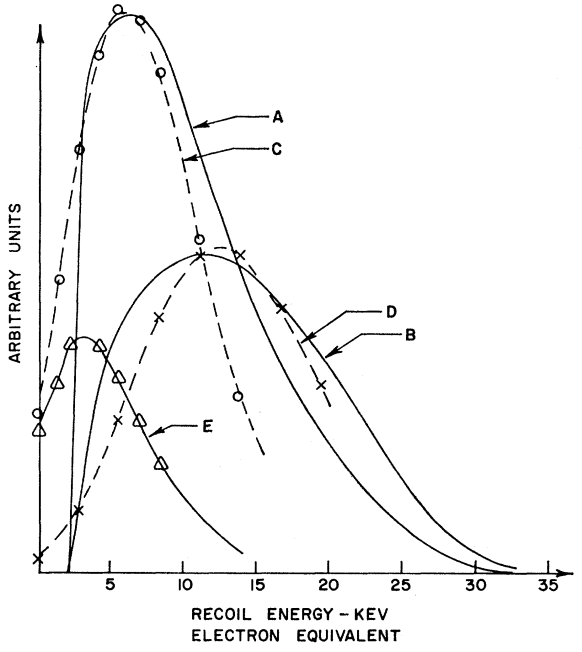

FIG. 11. Curves A and B: Observed x-ray energy spectra for 8- and 15-keV x rays, respectively. The sources were in solution in liquid scintillant (counter No. 5) and coincidence with a nuclear γ ray was required. Curves C and D: Best fits of Poisson distribution $P_m(x)$ to curves A and B where m and the scale of x were the fitted parameters.

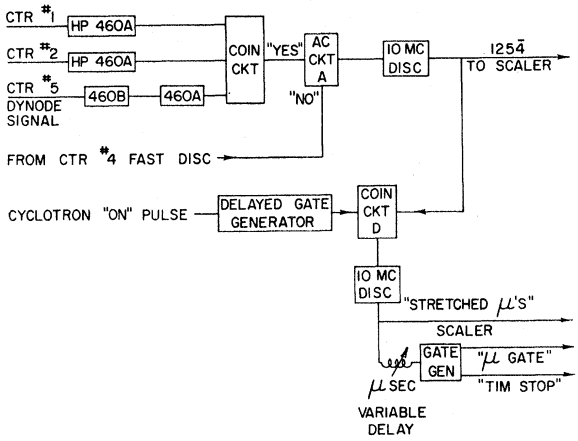

FIG. 12. Block diagram of monitor circuit for experiment to measure absorption to excited states of B^{12}.

In addition to its role in the fast-coincidence circuit E, the gamma-ray signal from No. 6 was amplified for pulse-height analysis. Circuit F gated the PHA for analyzing the No. 6 linear signals, if it simultaneously received (1) a signal from the linear amplifier on No. 6 indicating a γ ray in the energy region of interest, (2) the muon gate signal, and (3) the gated recoil $-\gamma$ coincidence output. The PHA gate signal was used to open the ADC of an RCL-256 channel analyzer. The ADC converted the linear γ-ray pulse to a signal which possessed a width proportional to the γ-ray energy. This width was measured by a 10 Mc/sec Hewlett-Packard time interval meter (TIM), and the measurement stored in the TIM scaling units. The "PHA gate" signal started a second TIM which was stopped (as mentioned above) by a pulse fixed in time relative to the stopping of the muon. The two TIM's thus stored both the time and pulse height of each recoil $-\gamma$ event, constituting a two-dimensional analyzer. This data was not recorded, however, unless a further condition involving the event was satisfied.

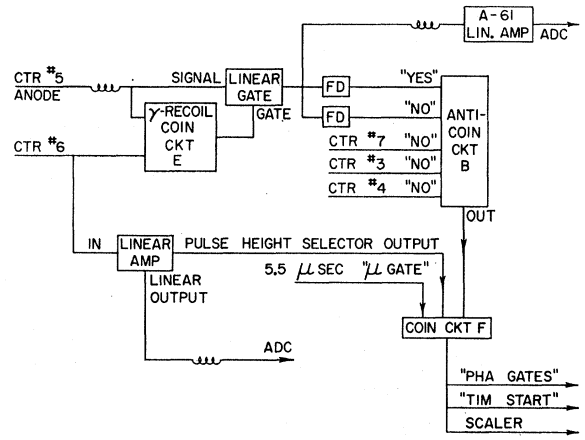

FIG. 13. Block diagram of circuitry for detection of gamma rays from excited states of B^{12}.

This last condition was the formation of a B^{12} nucleus, its ground state and its subsequent β decay. Referring again to Fig. 4, we note certain changes in the measurement of these β-decay electrons from the technique used in experiment I. They were made to optimize data-accumulation efficiency, and were:

(1) The cyclotron was operated for bursts of 4 FM pulses so that (t_1-t_0) was approximately 15 msec.

(2) There was a 12-msec delay between the last beam pulse and the start of the B^{12} gate to allow disappearance of machine associated background. Thus, (t_2-t_1) was approximately 12 msec.

(3) The counting gate (t_3-t_2) was narrowed to approximately 33 msec.

(4) Since the time for this complete cycle is about 60 msec, the repetition rate was increased to approximately 15/sec.

The analysis of the time and energy for a recoil-γ event occupied about 130 μsec. These two measurements were then displayed on two TIM scalers, and were printed as a single event *only* if a command signal to the printer was supplied. The command signal was generated by the occurrence of a PHA gate signal and of a B^{12} decay signal during a single cycle consisting of 4 cyclotron FM pulses and the following 33-msec B^{12} counting interval.

During the course of the experiment several different categories of data were recorded. Type I was accumulated for 58.35 h, and was as described above. That is, the energy of the γ ray and the time of the recoil $-\gamma$ coincidence were printed; the useful γ-ray energy interval was 0.8–1.9 MeV. Type II (23.27 h) substituted the energy of the recoil in No. 5 for the γ-ray energy. The time of the γ-recoil coincidence was recorded as in type I. The γ-ray energy which was accepted was 0.9 to 1.0 MeV, so that only the first excited state (0.95 MeV) of B^{12} was involved. In type-III data (29 h) a dual-beam oscilloscope was used to record recoil energy, γ-ray energy (0.8–3.0 MeV) and recoil $-\gamma$ time, providing three-dimensional analysis.

D. Data Analysis

The fraction B* of bound B^{12} formed in each of the excited states was evaluated as follows. Let:

$n_{ob}(E)$ = number of events of type I, II, or III as observed in an energy band having the appropriate instrumental width at the energy E.

N = number of stopping particles associated with $n_{ob}(E)$.

$F(E)$ = fraction of counts included in the FWHM of a Gaussian distribution. For a single Gaussian peak, $F=0.76$, and for the adjacent unresolvable peaks at 2.62 and 2.72 MeV, we obtained $F=0.87$.

T_μ = detection efficiency arising from finite gate width.

$\epsilon\Omega(E)/4\pi$ = geometrical and photopeak efficiency for observing γ rays in counter No. 6.

ϵ^γ = efficiency for detecting γ-recoil coincidence $=0.75\pm0.25$.

g_B = number of B^{12} nuclei produced per stopping particle.

η_B = efficiency for observing B^{12} decays, taking into account spectral loss, surface escape, etc.

R = efficiency for detecting recoil in No. 5, which is less than unity because of the 2.6 keV cutoff on the spectrum accepted.

Upon taking into account the effects of the cyclotron program used in the excited-state measurement, it is found that

$$B=\frac{R}{F(E)}\frac{n_{ob}{}^{(E)}}{N}\frac{4.43}{\epsilon\Omega(E)/4\pi}\frac{1}{\epsilon^\gamma g_B\eta_B}. \tag{6}$$

The factor $g_B\eta_B$ was measured as in experiment I, and found to have a value $(5.59\pm0.29)\times10^{-3}$.

We now discuss the evidence that the events which we attribute to excited state B^{12} production via reaction (1a) in fact proceeded from this cause. In Fig. 14, curve A represents the integral (!) time distribution of all recoil $-\gamma$ coincidences of type I, II, and III. The measured mean life is 2.0 μsec, within error ($\sim$7%) equal to the carbon muon lifetime of 2.04 sec. Curve B is an integral time spectrum of the events which have $\sim$0.95 MeV γ energy and $\leq$26 keV recoil energy. The low value of 1.8 μsec is acceptable, in view of the poor statistics. We are thus assured that the observed events

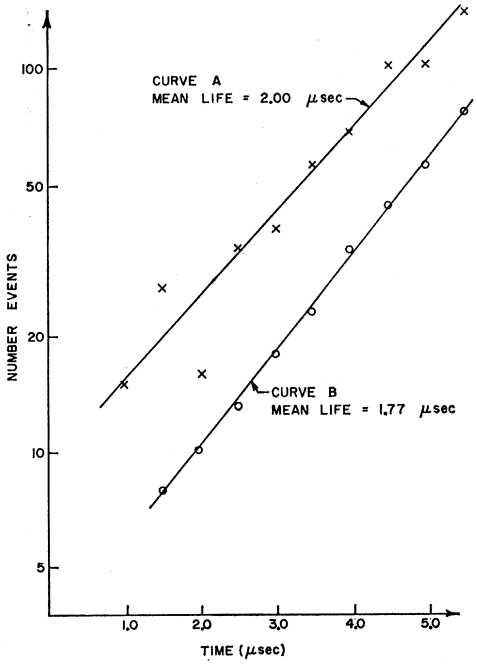

FIG. 14. Curve A: Time spectrum of all events, data types I, II, III. Curve B: Integral time spectrum of "good" events (0.95-MeV γ, recoil $\leq$26 keV).

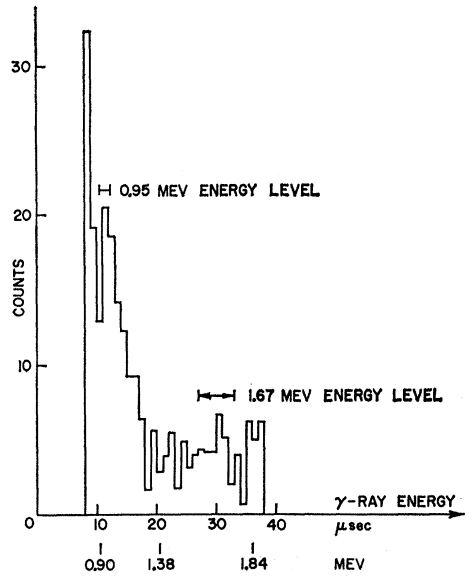

FIG. 15. γ-energy spectrum of type I data and low-energy portion of type III data, summed over all times within "μ gate."

were associated with stopping muons in carbon. No further use could be made of the time information for each event, and in the following discussion the data from all times within the muon gate are considered together.

Figure 15 shows that portion of the γ-energy spectrum of all types I and III events between 0.8 and 1.9 MeV. We ascribe a large portion of the events in the 0.95-MeV region to de-excitation of the first excited state in B^{12}. Note the limits indicated for the FWHM points for 0.95 and 1.67 MeV, as deduced from measurements with the calibration gamma rays of Na^{24} and Y^{88} with energies indicated on the horizontal axis. Although the 0.95-MeV γ ray is the only one of the excited states for which positive evidence exists in the date of Fig. 15, we admit the possibility of some contribution in the 1.67-MeV region, in view of the limited accuracy with which background can be deduced from the few events in the neighborhood of this region.

Further indication of the reality of the events in the 0.95-MeV region, as well as a measure of the background at this energy, is provided by study of the recoil pulse heights displayed in Fig. 16. Histogram A includes all

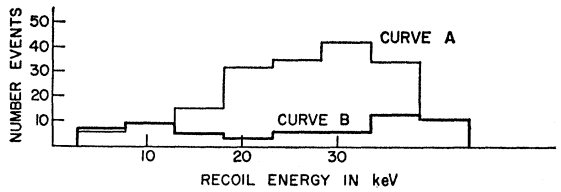

FIG. 16. Curve A: Spectrum of recoil pulse heights associated with 0.95-MeV gamma rays, for data types II and III, summed over. Curve B: Recoil pulse-height spectrum of type III, for *all* gamma-ray energies, *other than* 0.95 MeV, summed over time.

TABLE VI. Summary of numbers of events observed for various energy conditions on the recoil and gamma ray (see text).

Gamma-ray interval (MeV)	Stretched μ's$\times 10^{-6}$	Recoil energy range (keV)	Data group	n_0	R
0.90–1.0	15.2	...	I & III	39.1	
0.85–1.05	9.29	≥ 26	II & III	34	
0.85–1.05	9.29	<26	II & III	29	0.48±0.11
0.85–1.05	9.29	<18	II & III	21	0.34±0.09
1.59–1.75	5.12	≥ 26	III	5	
1.59–1.75	5.12	<26	III	4	0.44±0.29
1.59–1.75	5.12	<18	III	4	0.44±0.29
2.49–2.86	5.12	≥ 26	III	6	
2.49–2.86	5.12	<26	III	3	
2.49–2.86	5.12	<18	III	1	

types II and III data regardless of γ-ray energy, while histogram B includes only those events with gamma-ray energy $\sim$0.95 MeV. Comparison shows that the 0.95 MeV events show a much larger fraction of recoils in the low (<25 keV) region of the spectrum than do the events as a whole. This is what we should expect of excited state counts, as indicated by the curves of Fig. 11. One may ask, however, why the histogram A in Fig. 16 shows a background of high energy (>20 keV) recoils in number competitive with the lower energy recoils. These higher energy recoils are attributed to accidental coincidence between recoil $-\gamma$ events and B^{12} decay electron. The recoil $-\gamma$ coincidences could be generated by $B^{12*} \rightarrow B^{11*} + n \rightarrow B^{11} + n + m\gamma$, where $m \geq 1$. Thus, the "recoil" in No. 5 was often a gamma ray from the de-excitation of a B^{11*} nucleus produced via muon absorption to unbound B^{12} states. We also observed that the absolute rate of all recoil $-\gamma$ coincidences (without B^{12} β-decay condition) was comparable to the total absorption rate of muons in carbon, which is about what one would expect from the large number of states in B^{11}.

Thus, we use the histogram A of Fig. 16 to estimate the background under the 0.95-MeV peak in Fig. 15, by using a recoil energy cutoff of 26 keV. We conclude that approximately half of all observed events with γ-ray energies of 0.95 MeV are real. The actual values for the quantity R are given in Table VI. In sum we observed 13±4 recoil $-\gamma$ coincidences from the decay of the 0.95-MeV state of B^{12} formed by muon capture in C^{12}. Taking into account the efficiencies from Fig. 10, and measured values for the other quantities in Eq. (6), we tabulate in Table VII the fraction of B^{12} events

TABLE VII. Values of B* for the bound states of B^{12}.

Energy level MeV	B* (%) for upper limit on recoil energy of 18-keV electron equivalent
0.95	4.33±1.96
1.67	6.00±3.18
2.67	1.47±2.16

per bound B^{12} nucleus formed by muon capture in carbon. Because no peak was resolved for any of the levels above 0.95 MeV, it is felt that the numerical values in Table VIII for B*(1.67) and B*(2.67) should be regarded as upper limits.[21] The large statistical errors and uncertainty (33%) in ϵ^γ dominate the errors in Table VII, which include an estimate of systematic errors.

IV. RESULTS AND DISCUSSION

A. Experimental Results

The rate of reaction (1a) can now be obtained by combining the results of Secs. II and III. Recall that B is the partial muon capture rate for formation of bound B^{12}, expressed as a fraction of the number of muons which decay. The decay rate of muons bound in the K orbit of a carbon nucleus is known to be the same (within 0.2%) as that for free positive muons.[13] We can therefore use the measured decay rate of positive muons $\lambda_\mu^{\text{free}}$, to calculate λ_B^{gnd} according to the relation

$$\lambda_B^{\text{gnd}} = B\lambda_\mu^{\text{free}}[1-\sum B^*], \tag{7}$$

where $(\sum B^*)$ is the sum of the partial capture fractions to each of the excited states. Due to the large uncertainties in B*(1.67) and B*(2.67), we prefer to consider them as corrections to the lower deviation of λ_B^{gnd}. Thus B*(0.95) is used alone in Eq. (7). The final result is:

$$\begin{aligned}\lambda_B^{\text{gnd}} &= (1.55\pm0.06)\times10^{-2}\times0.962\pm0.021)\times\lambda_\mu^{\text{free}} \\ &= (6.75\pm_{0.75}^{0.30})\times10^3\ \text{sec}^{-1},\end{aligned} \tag{8}$$

where the lower deviation has been increased by $\lambda_B^{\text{gnd}}\times[B^*(1.67)+B^*(2.67)]$. All experimental results other than the present one are listed in Table VIII, where the values include a 10% correction for capture to excited states, but the errors quoted *do not* include a contribution from the uncertainty in the correction factor.

Two possible small contributions to the observed B^{12} rate have not yet been discussed. They are associated with the content of C^{13} in any carbon sample, which gives rise to the reactions

$$\mu^-+C^{13}\rightarrow B^{12}+n+\nu, \tag{9}$$

$$\mu^-+C^{13}\rightarrow B^{13}+\nu. \tag{10}$$

We estimate that 7% of muons captured in C^{13} mesonic atoms will undergo reaction (9). Taking into account the 1% abundance of C^{13}, the total production rate of B^{12} in counter No. 5 via reaction (9) is 7×10^{-4} *per stopped muon*. When compared to the production rate of B^{12} via reaction (1) of 1.5×10^{-2} per stopped muon, the contribution of reaction (9) to the B^{12} rate is concluded to be about 5%. This correction has *not* been made to the value given in (8) because of lack of experimental information. Reaction (10) leads to the beta decay of B^{13} ($t_{1/2}\sim35$ msec, end-point energy 13.4 MeV)[15] which would be indistinguishable from that of B^{12}. Assuming comparable rates for reactions (1) and (10), the isotopic abundance of C^{13} reduces the contribution from (10) to the 1% level, and it can be ignored.

We are in essential agreement with the Los Alamos group[8] about the magnitude of the excited-state contribution. They observed 21 events occurring within a few μsec after the muon stop and associated with delayed signals of approximately the B^{12} lifetime. Our events showed not only these characteristics, but also possessed γ-ray and recoil energies appropriate to the known character of B^{12*} and the muon capture kinematics.

However, the discrepancies between the B^{12} production rates measured at both Los Alamos[8] and CERN[6] and the rates measured by all other experimenters are deserving of comment. The Los Alamos result includes an error involving only statistical contributions, so that systematic effects might still be present. It has also been suggested to us[22] that the flux of cosmic-ray protons is sufficient to produce enough N^{12} through $C^{12}(p,n)N^{12}$ to seriously affect the Los Alamos muon capture experiment. If the (p,n) reaction cross section is of the order of millibarns, the proton flux is high enough to cause an appreciable N^{12} component in the B^{12} decay curve, and with only 512 decay events in all, the presence of the N^{12} (16.5 msec$=\tau$) may not have been detected.

With regard to the CERN experiment, it also seems likely that a short-lived component of activity was present in the B^{12} decay curve, which would result in an apparently large B^{12} amplitude. As we have detailed above in Sec. II, such contamination is easy to overlook. Finally, the pure muon beam used in the experiment reported here produced a B^{12} activity almost entirely due to muons, without measurable contamination from $C^{12}(n,p)B^{12}$. Thus, we were able to avoid complicated background extrapolation and subtraction techniques. We may also remark that in the two experiments[9,10] which measured reaction (1) with visual techniques, false activities are eliminated by geometrical identifica-

TABLE VIII. Results of earlier measurements of λ_B^{gnd}.

Experiment	$\lambda_B^{\text{gnd}}\times10^{-3}$ sec
T. N. K. Godfrey (Ref. 5)	5.9 ±1.5
J. O. Bergman *et al.* (Ref. 6)	9.18±0.5
F. B. Harrison *et al.* (Ref. 8)	9.05±0.95
B. L. Bloch (Ref. 7)	5.8 ±1.3
J. G. Fetkovich *et al.* (Ref. 9)	6.8 ±1.1
G. T. Reynolds *et al.* (Ref. 10)	6.7 ±0.9

[21] M. Ruel and J. G. Brennan [Phys. Rev. **129**, 866 (1963)] have performed shell model calculations of the muon capture rates to bound excited states of B^{12}. Their results are in fair agreement with this experiment, except for the 1.67-MeV state.

[22] J. Keuffel (private communication).

tion of a B^{12} decay with a stopping muon. Both experiments yielded results compatible with those of the present experiment.

B. Comparison of Results with Theory

It was remarked in the Introduction that the rate for reaction (1) is determined by the *effective* G-T coupling constant (2), which itself involves the various muon capture coupling constants which one would like to determine. Thus, the measurement of one number, the rate $\lambda_B{}^{gnd}$, cannot determine all these coupling constants. So the various theoretical calculations have all made the standard assumptions which are outlined in the Introduction, and then measured the effect of varying the g values, e.g., letting $g_P{}^\mu = -8g_A{}^\mu$, leaving out the weak magnetism $g_M{}^\mu$, etc. Among the theoretical papers, those of Wolfenstein,[23] Morita and Fujii,[24] and Flamand and Ford[25] are similar in that all three papers consider the allowed, second-forbidden, and relativistic contributions of the axial vector interactions, as well as the second-forbidden contributions of g_P and g_V. Wolfenstein and Morita and Fujii used the j-j coupling shell model, while Flamand and Ford used the intermediate coupling model. In addition, the latter used the charge distribution of C^{12} from electron scattering, which alters the muon S-state wave function from that for a point charge nucleus and thus results in a 6% reduction in B^{12} reaction rate. This correction should be made to the results of Wolfenstein and of Morita and Fujii, in which case the three calculations with the "canonical" assumptions of Sec. I yield transition rates:

$$\begin{aligned} \lambda_B{}^{gnd} &= 6810 \pm 817\,,^{25,26} \\ &= 6956 \pm 1600\,,^{23} \\ &= 6693 \pm 1600.^{24} \end{aligned} \tag{11}$$

The errors in the last two values are based on an estimate by Wolfenstein of the inaccuracies in the nuclear wave functions. The error assigned by Flamand and Ford is the result of a study of the sources of theoretical uncertainty made in Sec. V of their paper, and amounts to $\pm 12\%$, where Wolfenstein has about 20%.

Flamand and Ford showed that the transition rate is most sensitive to changes in $g_A{}^\mu$, with a 1% change in this parameter causing 1.7% change in transition rate. The sensitivity to changes in B^{12} nuclear radius was about half as great as that to $g_A{}^\mu$, sensitivity to $g_V{}^\mu$ one-fifth as great, and sensitivity to $g_P{}^\mu$ one-twentieth as great. The essence of their error studies is that one cannot expect to determine the coupling constants well, except for $g_A{}^\mu$, which is already deducible from $\pi - e$ decay. Thus, the excellent agreement between the theoretical results (11) and the experimental result (8) is evidence in support of UFI but cannot serve to place stringent limits on coupling constants.

We note, however, that if we (a) omit the weak magnetism term $g_M{}^\mu$, still keeping $g_P{}^\mu = +8g_A{}^\mu$, or (b) let $g_P{}^\mu = -8g_A{}^\mu$, keeping $g_M{}^\mu = 3.7g_V{}^\mu$, or (c) let $g_P{}^\mu = +16g_A{}^\mu$, keeping $g_M{}^\mu = 3.7g_V{}^\mu$, or (d) let $g_P{}^\mu = g_M{}^\mu = 0$, then the theoretical values become (a) 5300 sec^{-1}, (b) 9800 sec^{-1}, (c) 6300 sec^{-1}, and (d) 6200 sec^{-1}, all with 10–15% theoretical uncertainty. Only the last two values fall within our experimental error. We note that a negative value for $g_P{}^\mu/g_A{}^\mu$ is much less favored than a positive value. This is in agreement with the results of neutron asymmetry measurements[27] and a recent experiment on muon capture in O^{16}.[28] If the value of $g_P{}^\mu/g_A{}^\mu$ is assumed to lie between 5 and 20, which is consistent with these experiments, then our result on the B^{12} rate favors the presence of the weak magnetism term.

In summary, we observe that the experimental data yields a transition rate of reaction (1) in good agreement with the universal weak interaction theory, and with an uncertainty considerably less than that in current theoretical calculations.

We are indebted to Professor L. Wolfenstein for his comments and exposition of theoretical aspects of weak interactions.

[23] L. Wolfenstein, Nuovo Cimento **13**, 319 (1959).
[24] M. Morita and A. Fujii, Phys. Rev. **118**, 606 (1960).
[25] G. Flamand and K. W. Ford, Phys. Rev. **116**, 1591 (1959).
[26] We have quoted here the second UFI value appearing in Table II of Ref. 25, i.e., the transition rate calculated using the theoretical vector matrix element. The first value in this table is generally quoted, and is based on the "experimental" vector matrix element. However, Flamand and Ford already pointed out, in a note added in proof to Ref. 24, that the experimental data on which this first rate was based had been superceded by later results, which brought the "experimental" vector matrix element down to the theoretical value. Thus the rate of 6810 sec^{-1} quoted here is to be preferred for good reason, aside from its better agreement with our experiment.
[27] A. Astbury, J. M. Blair, M. Hussain, M. A. R. Kemp, H. Muirhead, R. G. Voss, Phys. Rev. Letters **3**, 476 (1959); V. L. Telegdi, in *Proceedings of the 1960 Annual International Conference on High-Energy Physics at Rochester* (Interscience Publishers, Inc., New York, 1960), p. 713; V. S. Evseev, V. I. Komarov, V. Z. Kush, V. S. Roganov, V. A. Chrnogorova, and M. M. Szymczak, Zh. Eksperim. i Teor. Fiz. **41**, 306 (1961) [translation: Soviet Phys.—JETP **14**, 217 (1962)].
[28] R. C. Cohen, S. Devons, and A. D. Kanaris, Phys. Rev. Letters **11**, 134 (1963).